



Article scientifique

Article

2009

Published version

Open Access

This is the published version of the publication, made available in accordance with the publisher's policy.

Electric-field tuning of the metal-insulator transition in ultrathin films of LaNiO₃

Scherwitzl, Raoul; Zubko, Pavlo; Lichtensteiger, Céline; Triscone, Jean-Marc

How to cite

SCHERWITZL, Raoul et al. Electric-field tuning of the metal-insulator transition in ultrathin films of LaNiO₃. In: Applied physics letters, 2009, vol. 95, n° 22, p. 222114. doi: 10.1063/1.3269591

This publication URL: <https://archive-ouverte.unige.ch/unige:23385>

Publication DOI: [10.1063/1.3269591](https://doi.org/10.1063/1.3269591)

Electric-field tuning of the metal-insulator transition in ultrathin films of LaNiO₃

R. Scherwitzl, P. Zubko, C. Lichtensteiger, and J.-M. Triscone

Citation: *Appl. Phys. Lett.* **95**, 222114 (2009); doi: 10.1063/1.3269591

View online: <http://dx.doi.org/10.1063/1.3269591>

View Table of Contents: <http://apl.aip.org/resource/1/APPLAB/v95/i22>

Published by the [American Institute of Physics](http://www.aip.org).

Related Articles

Heteroepitaxial VO₂ thin films on GaN: Structure and metal-insulator transition characteristics

J. Appl. Phys. **112**, 074114 (2012)

Pressure dependence of the Verwey transition in magnetite: An infrared spectroscopic point of view

J. Appl. Phys. **112**, 073524 (2012)

Temperature induced delocalization of charge carriers and metallic phase in Co_{0.6}Sn_{0.4}Fe₂O₄ nanoparticles

J. Appl. Phys. **112**, 063718 (2012)

Negligible carrier freeze-out facilitated by impurity band conduction in highly p-type GaN

Appl. Phys. Lett. **101**, 082106 (2012)

Anderson localization in strongly coupled gold-nanoparticle assemblies near the metal-insulator transition

Appl. Phys. Lett. **101**, 083105 (2012)

Additional information on *Appl. Phys. Lett.*

Journal Homepage: <http://apl.aip.org/>

Journal Information: http://apl.aip.org/about/about_the_journal

Top downloads: http://apl.aip.org/features/most_downloaded

Information for Authors: <http://apl.aip.org/authors>

ADVERTISEMENT

AMERICAN
PHYSICAL
SOCIETY'S
OPEN ACCESS
JOURNAL

PRX

Committed to
Excellence

Physical Review X
prx.aps.org

Electric-field tuning of the metal-insulator transition in ultrathin films of LaNiO_3

R. Scherwitzl,^{a)} P. Zubko, C. Lichtensteiger, and J.-M. Triscone
DPMC, University of Geneva, 24 Quai Ernest-Ansermet, 1211 Genève 4, Switzerland

(Received 18 September 2009; accepted 8 November 2009; published online 4 December 2009)

Epitaxial ultrathin films of the metallic perovskite LaNiO_3 were grown on (001) SrTiO_3 substrates using off-axis rf magnetron sputtering. The film structure was characterized and their electrical properties investigated. Films thinner than 8 unit cells display a metal-insulator transition at a thickness dependent characteristic temperature. Hall measurements revealed p-type conduction, which was confirmed by electric field-effect experiments. Large changes in the transport properties and the metal-insulator transition temperature were observed for the thinnest LaNiO_3 films as the carrier density was electrostatically tuned. © 2009 American Institute of Physics.
 [doi:10.1063/1.3269591]

The perovskite nickelates (RNiO_3 , where R is a rare earth) are a fascinating family of compounds that display sharp temperature-driven metal-insulator (M-I) transitions with resistance changes of up to four orders of magnitude.^{1,2} The conduction band is believed to be formed by the overlap of the Ni d orbitals and the O p orbitals. This overlap is structurally correlated with the ionic radii of the rare earths and influenced by the temperature. With decreasing temperatures, the NiO_6 octahedra buckle and the reduced overlap is thought to induce the M-I transition.^{3,4} The precise mechanism for the gap opening, however, is still under debate, with the most recent data showing that charge disproportionation ($2\text{Ni}^{3+} \rightarrow \text{Ni}^{3+\delta} + \text{Ni}^{3-\delta}$) with an accompanying symmetry change from orthorhombic to monoclinic may be at the origin of the localization for the entire RNiO_3 series.^{5,6} To date, the most technologically relevant of the nickelates is LaNiO_3 . It is the only member of the family that does not display a M-I transition in its bulk form, remaining metallic down to the lowest temperatures. Bulk and thin films of this metallic oxide have been studied extensively in the past⁷⁻⁹ and LaNiO_3 is a popular choice as an electrode material in oxide electronics. For instance, in the area of ferroelectric memories and devices, the use of conducting perovskite oxides such as LaNiO_3 and SrRuO_3 allows coherent growth of fully strained epitaxial perovskite thin films and is believed to improve device properties. One should also note that very thin oxide metallic films are of importance in devices with a low strain budget that require the thinnest possible electrodes. The metallicity of thin films can however be affected by several parameters. It was reported that a M-I transition can take place in LaNiO_3 if the amount of disorder is sufficiently increased, e.g., by introducing oxygen vacancies.¹⁰ In this letter, we show that epitaxial LaNiO_3 thin films grown coherently on (001) SrTiO_3 exhibit a M-I transition as the film thickness is reduced below 8 unit cells (u.c.). The transition temperature T_{MI} was found to be tunable by up to 24 K using the electric field effect and resistivity changes of up to 10% were observed. The successful field tuning of the T_{MI} in LaNiO_3 paves the way to orders of magnitude larger field-induced resistivity changes that should be achievable by ex-

ploiting the intrinsic M-I transition of the other RNiO_3 compounds, and hence to the possibility of electronic devices based on nickelate thin films.¹¹ In addition, the field effect measurements, as well as Hall effect studies, reveal p-type conduction in our LaNiO_3 thin films, in contrast to previously published reports.

The primitive cell of bulk LaNiO_3 is rhombohedral, with lattice parameter $a=5.46 \text{ \AA}$, and rhombohedral angle $\alpha=60.49^\circ$. It is well approximated by a pseudocubic cell with $a=3.84 \text{ \AA}$.¹² The LaNiO_3 films thus experience tensile strain when grown on SrTiO_3 ($a=b=3.905 \text{ \AA}$) due the 1.7% lattice mismatch between the two materials. The growth of LaNiO_3 thin films onto (001) insulating SrTiO_3 substrates was carried out by off-axis rf magnetron sputtering in 0.180 mbar of an oxygen/argon mixture of ratio 1:3 at a substrate temperature of 510 °C. Epitaxial c-axis oriented LaNiO_3 films with thicknesses ranging from 4 u.c. to more than 75 u.c. were successfully grown using these conditions. It was found that the LaNiO_3 lattice parameters, as well as the presence of parasitic phases, depend strongly on the oxygen stoichiometry which could be controlled either by changing the partial oxygen pressure during growth or by postannealing the samples in oxygen.

Detailed x-ray measurements were performed with a high-resolution PANalytical X'Pert PRO diffractometer using the $\text{Cu } K\alpha_1$ radiation. The θ - 2θ scans around the (001) SrTiO_3 and LaNiO_3 diffraction peaks for samples with different thicknesses were obtained with a triple axis detector and are shown in Fig. 1(a). Finite size Fresnel oscillations were observed around the diffraction peak and simple fits to these curves allow the thickness and c-axis lattice parameter of the films to be obtained. The lattice parameter was found to be $\sim 3.80\text{--}3.81 \text{ \AA}$ for all the samples measured. The thickness obtained was also confirmed by reflectometry measurements. Atomic force microscopy (AFM) investigations of the film surfaces revealed atomically smooth terraces separated by a step height of 1 u.c. [see inset of Fig. 1(a)]. The full width at half-maximum of the rocking curves matched the one of the substrates. Finally, reciprocal space maps were made with a pixel detector to investigate the coherence of the LaNiO_3 films grown onto the SrTiO_3 . Measurements around the $(\bar{1}03)$ diffraction peaks for the film and the substrate, Fig. 1(b), showed that the in-plane lattice pa-

^{a)}Electronic mail: raoul.scherwitzl@unige.ch.

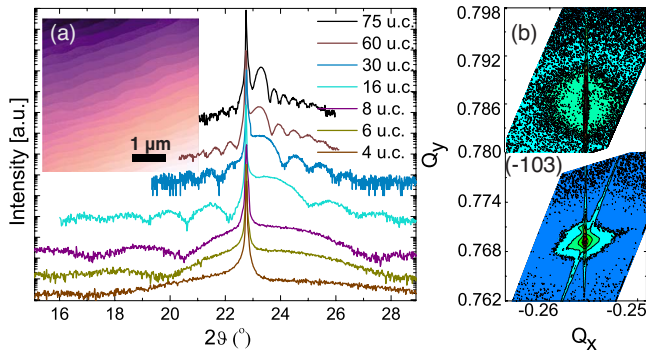


FIG. 1. (Color online) (a) θ - 2θ diffractograms for a series of LaNiO_3 films grown on (001) SrTiO_3 with thicknesses ranging from 4 to 75 u.c. The inset shows a $5 \times 5 \mu\text{m}^2$ AFM scan of a typical film surface. (b) Reciprocal space map around the $(\bar{1}03)$ reflection with $Q_x = h/a$ and $Q_y = l/c$ obtained on a 30 u.c. thick sample.

parameter of the LaNiO_3 layer was equal to the one of the SrTiO_3 substrate for all films investigated.

Electrical resistivity measurements ($30 \text{ mK} < T < 300 \text{ K}$), Hall measurements ($1.5 \text{ K} < T < 260 \text{ K}$) and field-effect studies were performed on films of different thicknesses. For the resistivity measurements, each sample was patterned in a way suitable for four-point resistance and Hall measurements and every measurement was reproduced on different locations of the $5 \times 5 \text{ mm}^2$ sample and on at least two other equivalent samples. The experimental geometry used is sketched in the inset of Fig. 2. Figure 2 shows the observed behavior from room temperature down to 4.2 K. For samples thicker than 7 u.c. the resistivity drops by nearly a factor of 3 from a room temperature value ranging from 280 to $400 \mu\Omega \text{ cm}$, to a residual resistivity typically found to be between 100 and $140 \mu\Omega \text{ cm}$, in agreement with previously published values.^{7,8} A 75 u.c. film was mounted in a dilution refrigerator enabling measurements down to 30 mK. The resistivity was found to be essentially constant between 4.2 K and 30 mK. I - V curves up to 1 mA showed linear behavior at all temperatures.

As the thickness of the films decreases below 8 u.c. a M-I transition can be observed. For 7 and 6 u.c. an upturn in

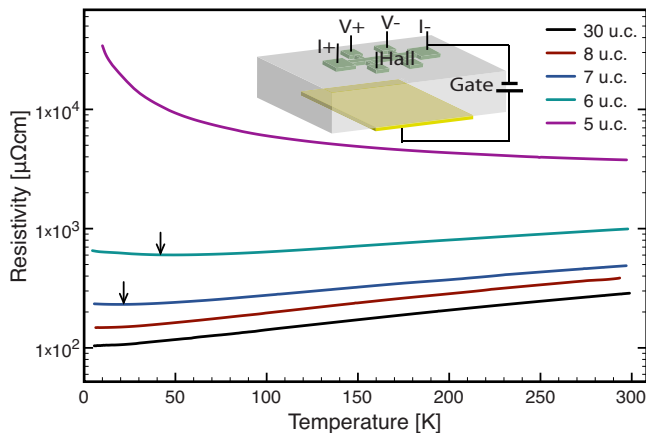


FIG. 2. (Color online) Temperature dependence of the resistivity for a series of LaNiO_3 films with thickness ranging from 5 to 30 u.c. A M-I transition is observed as the thickness is reduced. Arrows are indicating the onset of the M-I transition. The inset shows the geometry of the device, enabling four-point resistivity measurements, Hall measurements, and field effect experiments using a backgate configuration.

resistivity is observed, respectively, around 20 and 40 K, while for a thickness of 5 u.c. the behavior is insulating over the entire temperature range. Using the free electron model, the elastic scattering length in these thin films is found to be about $\sim 20 \text{ \AA}$, a value comparable to the thickness of the thinnest films.²⁵ An enhancement of the scattering at the film surface may contribute to the observed increase in resistivity. We note that rather similar M-I transitions have been observed in SrRuO_3 samples thinner than 4 u.c.^{15,16}

The nature of the observed M-I transition as a function of thickness is not at present understood. The simple explanation that the concentration of oxygen vacancies is larger near the interface with the substrate, thus increasing the relative fraction of nonstoichiometric material as films get thinner, seems unlikely due to lack of qualitative changes in behavior upon annealing the samples in oxygen. The weak localization scenario proposed to explain the M-I transition in bulk $\text{LaNiO}_{3-\delta}$ ^{17,18} combined with a progressive change in dimensionality as the sample thickness is reduced could explain the observed behavior. Further studies are however necessary to be able to draw firm conclusions on this point.

In order to elucidate the nature of charge carriers in LaNiO_3 films, Hall measurements were carried out from 1.5 to 260 K in a pumped He cryostat equipped with a superconducting magnet enabling magnetic fields up to 8 T. This setup also allows one to perform detailed magnetoresistance studies, which are currently underway and should help clarify the nature of the M-I transition. For samples thicker than 8 u.c. we obtain room temperature carrier densities of $\sim 2 \times 10^{22} \text{ cm}^{-3}$, a value close to the $1.7 \times 10^{22} \text{ cm}^{-3}$ expected if each Ni atom contributes one carrier. For thinner films, the charge density is gradually reduced to 1.5 and $1.0 \times 10^{22} \text{ cm}^{-3}$ for 7 and 6 u.c. samples, respectively. The carriers are found to be positive, i.e., holes rather than electrons, a result in contradiction with other studies.^{8,9,20} Indeed, previous work on bulk ceramics reports negative thermopower coefficients, concluding that electrons are the dominant charge carriers.^{8,9,19} Hall measurement data are scarce and less consistent. Noun *et al.*²⁰ report electronic transport with $n \approx 4 \times 10^{22} \text{ cm}^{-3}$ in their epitaxial films grown on SrTiO_3 , whereas Gayathri and co-workers¹⁷ measure a positive Hall coefficient, attributed to holelike pockets arising from charge transfer from the oxygen p to the metal d band. At the same time, Gayathri *et al.* also observe a negative Seebeck coefficient S . It is interesting to note that most of the previous measurements have been performed on either bulk ceramics or relaxed films with lattice parameters close to the bulk LaNiO_3 values. Our single crystalline films are lattice matched and fully strained to the substrate. First-principles calculations²¹ have shown that hypothetical cubic LaNiO_3 has a large hole Fermi surface, confirmed by recent photoemission measurements on tetragonal LaNiO_3 films.²² A setup for thermopower measurements is currently being developed in order to clarify this issue.

Another way to probe the nature of the carriers is to perform electric field-effect experiments, where the carrier density is modulated by applying an electric field between a gate and the conducting channel across a dielectric. Due to the large carrier density in LaNiO_3 , ultrathin films with thicknesses below 30 \AA are necessary to obtain substantial charge modulation.²³ In our field effect experiments, a backgate geometry was used, the dielectric being the SrTiO_3 substrate itself. The gate is a gold electrode deposited on

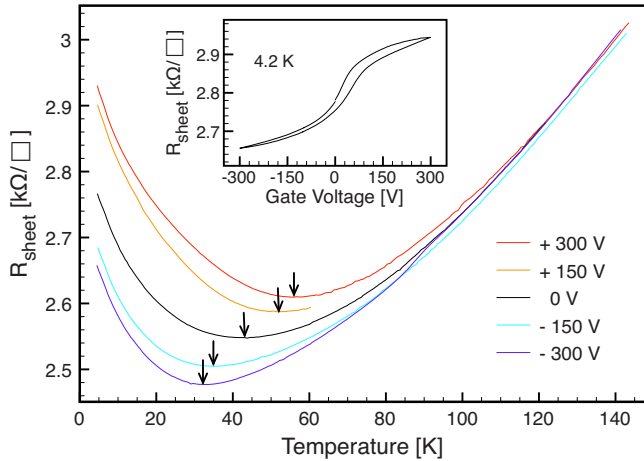


FIG. 3. (Color online) Sheet resistance R_{sheet} vs temperature for a 6 u.c. thick film and for different applied gate voltages. The inset shows the sheet resistance vs applied voltage at 4.2 K vs applied voltage at 4.2 K.

the backside of the substrate, opposite to the channel area. This configuration benefits from the high dielectric constant of SrTiO_3 , which increases substantially at low temperatures.^{13,14} The large thickness of the dielectric (0.5 mm) compared to the small width of the conducting channel (typically 10 to 100 μm) allows a further enhancement of the charge modulation due to the fringing field effect. Dynamic capacitance measurements as a function of gate voltage revealed that the average charge density modulation in the LaNiO_3 electrode was $\sim 8 \mu\text{C cm}^{-2}$ at 200 V and 4.2 K.

Figure 3 shows sheet resistance measurements for a 6 u.c. thick film and for gate voltages varying between -300 and 300 V. The inset shows the sheet resistance R_{sheet} versus applied gate voltage at 4.2 K. A change in R_{sheet} of $\sim 10\%$ from -300 to 300 V is observed, a large effect given the metallic nature of LaNiO_3 . We note that a similar magnitude was observed in field effect experiments performed on SrRuO_3 .²⁴ As can be seen, the resistance increases when a positive voltage is applied to the gate, which indicates that positive charge carriers are being removed from the LaNiO_3 layer, therefore agreeing with the p-type conduction observed in Hall measurements. A small hysteretic behavior appears, most likely due to charge trapping/detrapping in the substrate, but the device presents reproducible sheet resistance versus voltage and temperature characteristics. As mentioned above, 6 u.c. thick LaNiO_3 films exhibit a M-I transition at around 40 K. The sheet resistance versus temperature curves shown on Fig. 3 for different gate voltages reveal a shift of the transition temperature of up to 24 K. Defining T_{MI} as the temperature at which the resistance exhibits a minimum, T_{MI} is found to increase consistently with increasing the gate voltage from 42 K at 0 V to 56 K at 300 V, and to decrease down to 32 K at -300 V, showing that the metallic phase can be stabilized by the electric field over a relatively large temperature range. At higher temperatures, the decrease in the SrTiO_3 dielectric constant leads to a reduced charge modulation and the resistance is found to depend only weakly on applied voltage.

In conclusion, high-quality epitaxial LaNiO_3 thin films with thicknesses down to 4 u.c. were grown epitaxially and

coherently on (001) SrTiO_3 . It was found that the LaNiO_3 films are metallic down to 30 mK for films thicker than 7 u.c. Below this critical thickness, a M-I transition appears at 20 and 40 K for the 7 and 6 u.c. thick films, respectively, while a 5 u.c. thick film already displays a negative dR_{sheet}/dT at room temperature. Field-effect experiments performed on ultrathin films reveal a large resistivity and charge modulation of about 10% and directly indicate that coherent LaNiO_3 films grown on SrTiO_3 display p-type conduction, a result confirmed by Hall measurements. Finally, the M-I transition could be tuned by up to 24 K using an applied electric field.

We thank A. Caviglia, S. Gariglio, and M. Bavinck for help with transport measurements, N. Stucki and M. Lopes for technical support, and G. Catalan for fruitful discussions. This work was supported by the Swiss National Science Foundation through the National Center of Competence in Research, “Materials with Novel Electronic Properties, MaNEP” and division II.

¹G. Catalan, *Phase Transitions* **81**, 729 (2008).

²M. Medarde, *J. Phys.: Condens. Matter* **9**, 1679 (1997).

³J. Torrance, P. Lacorre, A. Nazzal, E. Ansaldo, and C. Niedermayer, *Phys. Rev. B* **45**, 8209 (1992).

⁴J. L. Garcia-Munoz, J. Rodriguez-Carvajal, and P. Lacorre, *Phys. Rev. B* **50**, 978 (1994).

⁵M. Medarde, M. T. Fernandez-Diaz, and P. Lacorre, *Phys. Rev. B* **78**, 212101 (2008).

⁶J. A. Alonso, J. L. Garcia-Munoz, M. T. Fernandez-Diaz, M. A. G. Aranda, M. J. Martinez-Lope, and M. T. Casais, *Phys. Rev. Lett.* **82**, 3871 (1999).

⁷K. Sreedhar, J. Honig, M. Darwin, M. McElfresh, P. Shand, J. Xu, B. Crooker, and J. Spalek, *Phys. Rev. B* **46**, 6382 (1992).

⁸K. Rajeev, G. Shivashankar, and A. Raychaudhuri, *Solid State Commun.* **79**, 591 (1991).

⁹X. Xu, J. Peng, Z. Li, H. Ju, and R. Greene, *Phys. Rev. B* **48**, 1112 (1993).

¹⁰M. Kawai, S. Inoue, M. Mizumaki, N. Kawamura, N. Ichikawa, and Y. Shimakawa, *Appl. Phys. Lett.* **94**, 082102 (2009).

¹¹J.-S. Zhou, J. B. Goodenough, B. Dabrowski, P. W. Klamut, and Z. Bukowski, *Phys. Rev. B* **61**, 4401 (2000).

¹²A. Wold, B. Post, and E. Banks, *J. Am. Chem. Soc.* **79**, 4911 (1957).

¹³D. Matthey, S. Gariglio, and J.-M. Triscone, *Appl. Phys. Lett.* **83**, 3758 (2003).

¹⁴T. Sakudo and H. Unoki, *Phys. Rev. Lett.* **26**, 851 (1971).

¹⁵J. Xia, W. Siemons, G. Koster, M. R. Beasley, and A. Kapitulnik, *Phys. Rev. B* **79**, 140407 (2009).

¹⁶Y. J. Chang, C. H. Kim, S.-H. Phark, Y. S. Kim, J. Yu, and T. W. Noh, *Phys. Rev. Lett.* **103**, 057201 (2009).

¹⁷N. Gayathri, A. Raychaudhuri, X. Xu, J. Peng, and R. Greene, *J. Phys.: Condens. Matter* **10**, 1323 (1998).

¹⁸G. Herranz, F. Sanchez, J. Fontcuberta, V. Laukhin, J. Galibert, M. Garcia-Cuenca, C. Ferrater, and M. Varela, *Phys. Rev. B* **72**, 014457 (2005).

¹⁹A. Tiwari and K. Raccach, *J. Phys.: Condens. Matter* **11**, 3291 (1999).

²⁰W. Noun, B. Berini, Y. Dumont, P. R. Dahoo, and N. Keller, *J. Appl. Phys.* **102**, 063709 (2007).

²¹N. Hamada, *J. Phys. Chem. Solids* **54**, 1157 (1993).

²²R. Eguchi, A. Chainani, M. Taguchi, M. Matsunami, Y. Ishida, K. Horiba, Y. Senba, H. Ohashi, and S. Shin, *Phys. Rev. B* **79**, 115122 (2009).

²³C. Ahn, J.-M. Triscone, and J. Mannhart, *Nature (London)* **424**, 1015 (2003).

²⁴C. Ahn, R. Hammond, T. Geballe, M. Beasley, J.-M. Triscone, M. Decroux, O. Fischer, L. Antognazza, and K. Char, *Appl. Phys. Lett.* **70**, 206 (1997).

²⁵The scattering length l was calculated as follows: $l = (mv_F)/(ne^2\rho) = (\hbar k_F)/(ne^2\rho)$, where $k_F = (3\pi^2 n)^{1/3}$. Using the values measured at 4.2 K for a 30 u.c. film ($\rho = 100 \mu\Omega \text{ cm}$ and $n = 1.5 \times 10^{22} \text{ cm}^{-3}$), we obtain $l \approx 20 \text{ \AA}$.